Deforming Composite Grids for Fluid Structure Interactions

Jeff Banks[1],
Bill Henshaw[1] ,
Don Schwendeman[2]

[1]Center for Applied Scientific Computing,
Lawrence Livermore National Laboratory, Livermore, CA, USA.

[2]Department of Mathematical Sciences,
Rensselaer Polytechnic Institute, Troy, NY, USA.

SIAM Conference on Computational Science and Engineering,
Reno, Nevada, February 28 - March 4, 2011.

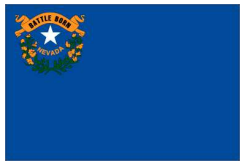

Acknowledgments.

Supported by:

ASCR Department of Energy, Office of Science, ASCR Applied Math Program .

LDRD LLNL: Laboratory Directed Research and Development (LDRD) program .

NSF National Science Foundation .

Outline

1. Background: overlapping grids, Overture and CG.
2. Deforming Composite Grids (DCG) for fluid structure interactions.
3. The elastic-piston problem and the fluid-solid Riemann problem.
4. Stable interface conditions for coupling the Euler equations and the elastic wave equation.
5. Verification problems.
    1. super-seismic shock
    2. deforming diffuser.

The Overture project is developing PDE solvers for a wide class of continuum mechanics applications.

Overture is a toolkit for solving PDE's on overlapping grids and includes CAD, grid generation, numerical approximations, AMR and graphics.

The CG (Composite Grid) suite of PDE solvers (cgcns, cgins, cgmx, cgsm, cgad, cgmp) provide algorithms for modeling gases, fluids, solids and E&M.

Overture and CG are available from www.llnl.gov/CASC/Overture.

We are looking at a variety of applications:

- wind turbines, building flows (cgins),
- explosives modeling (cgcns),
- fluid-structure interactions (e.g. blast effects) (cgmp+cgcns+cgsm),
- conjugate heat transfer (e.g. NIF holhraum) (cgmp+cgins+cgad),
- damage mitigation in NIF laser optics (cgmx).

Previous work: shock hitting rigid cylinders with AMR

(Shock hitting rigid cylinders with AMR)

randomCylRhoWithGrids.mpg

Current work: shock hitting elastic cylinders

(Shock hitting elastic cylinders)

shockMultiDisk.mpg

What are overlapping grids and why are they useful?

Overlapping grid: a set of structured grids that overlap.

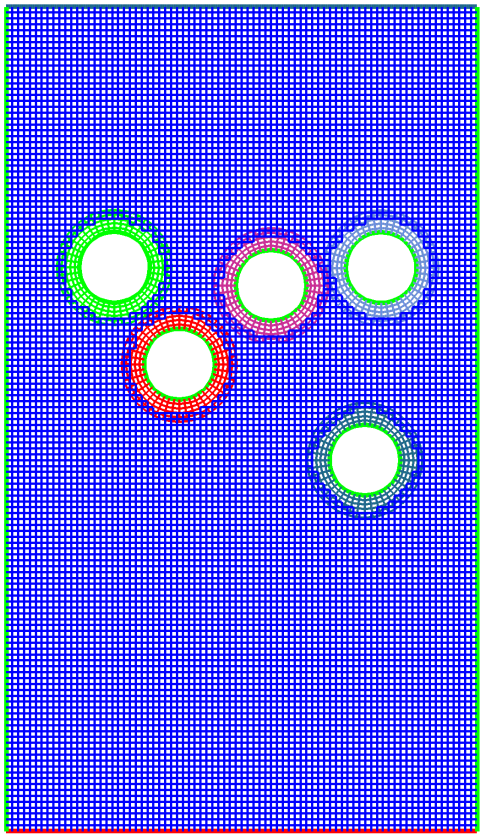

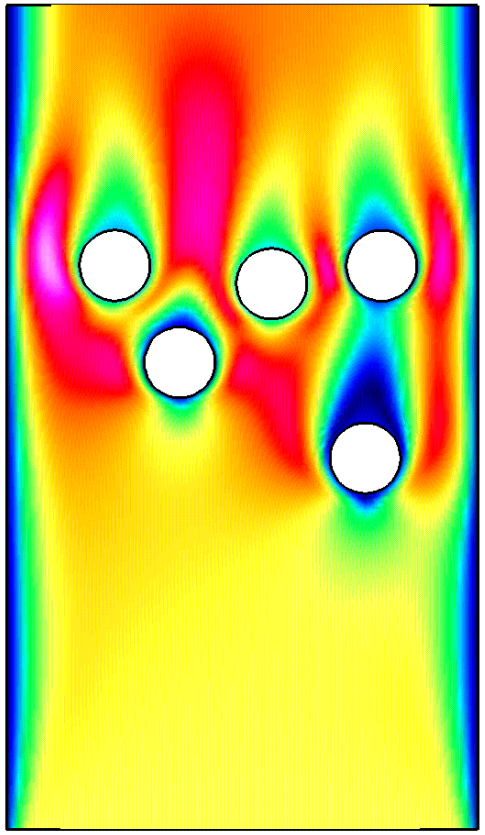

- Overlapping grids can be rapidly generated as bodies move.
- High quality grids under large displacements.
- Cartesian grids for efficiency.
- Efficient for high-order accurate methods.

What are overlapping grids and why are they useful?

Overlapping grid: a set of structured grids that overlap.

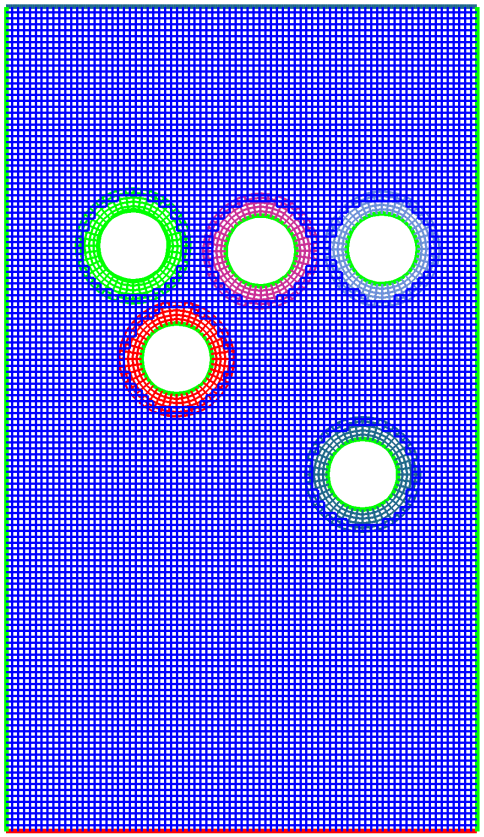

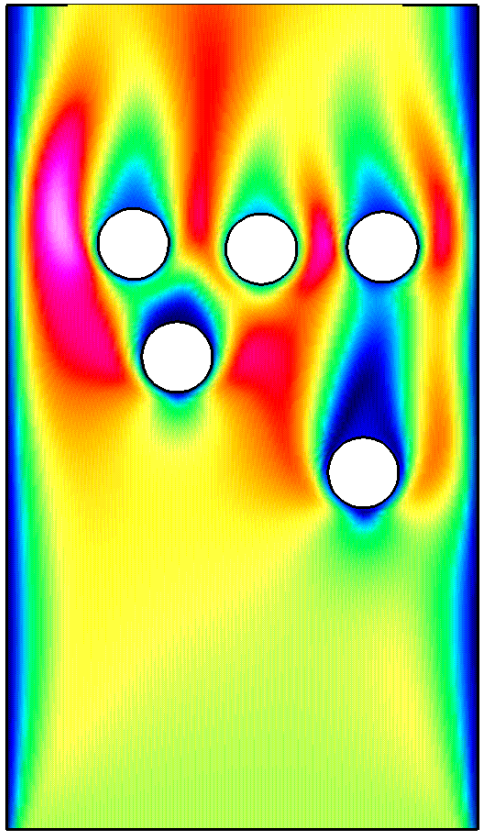

- Overlapping grids can be rapidly generated as bodies move.
- High quality grids under large displacements.
- Cartesian grids for efficiency.
- Efficient for high-order accurate methods.

What are overlapping grids and why are they useful?

Overlapping grid: a set of structured grids that overlap.

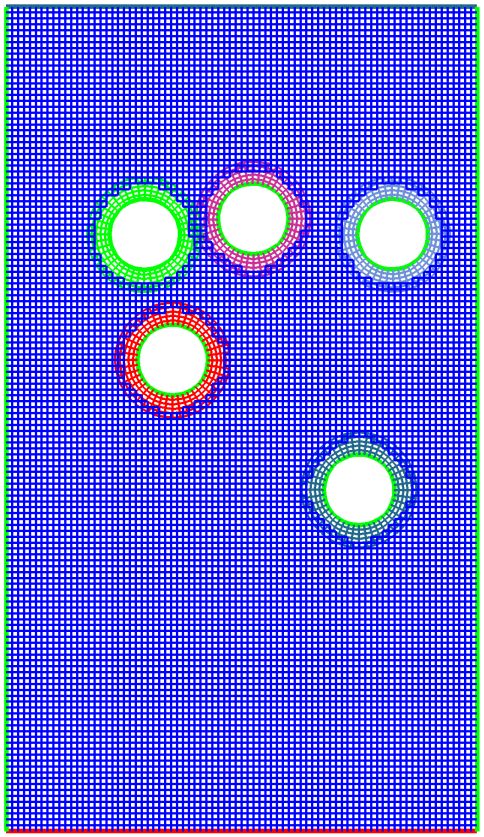

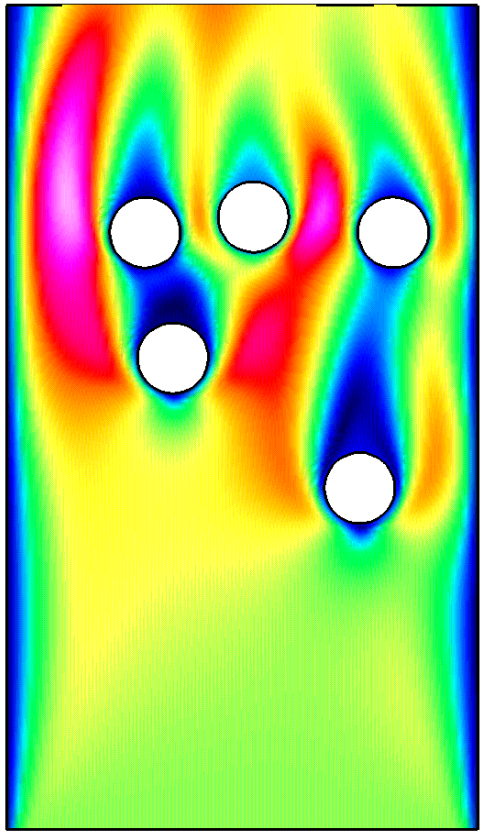

- Overlapping grids can be rapidly generated as bodies move.
- High quality grids under large displacements.
- Cartesian grids for efficiency.
- Efficient for high-order accurate methods.

What are overlapping grids and why are they useful?

Overlapping grid: a set of structured grids that overlap.

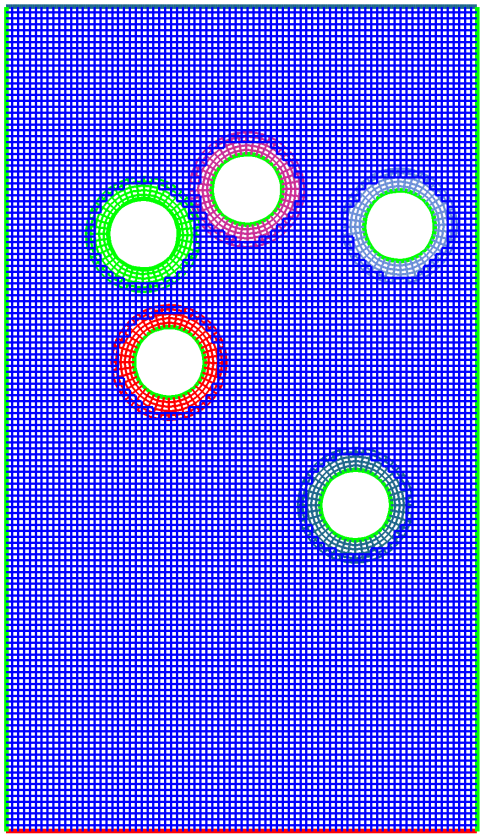

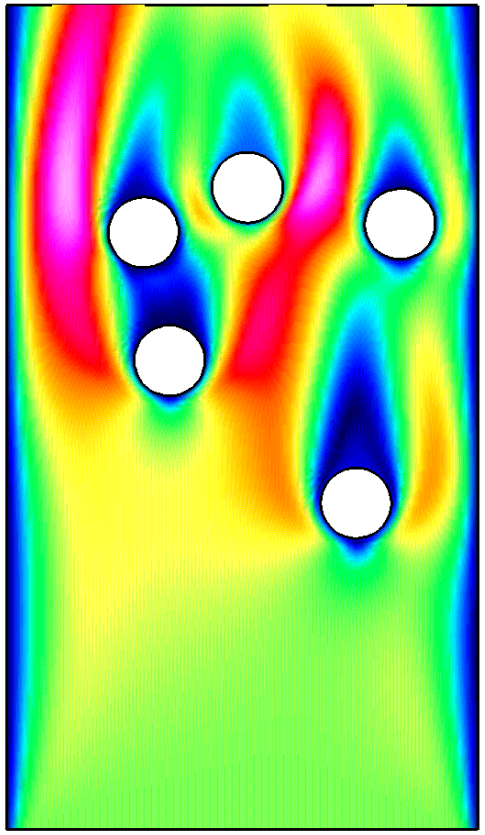

- Overlapping grids can be rapidly generated as bodies move.
- High quality grids under large displacements.
- Cartesian grids for efficiency.
- Efficient for high-order accurate methods.

What are overlapping grids and why are they useful?

Overlapping grid: a set of structured grids that overlap.

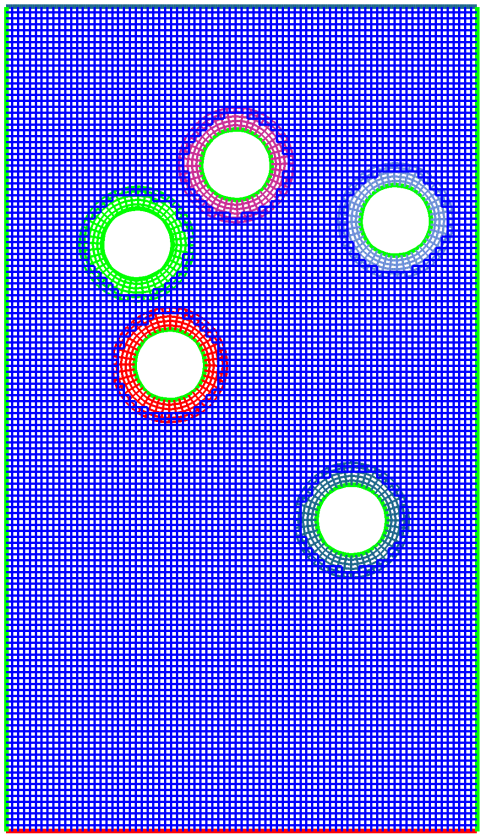

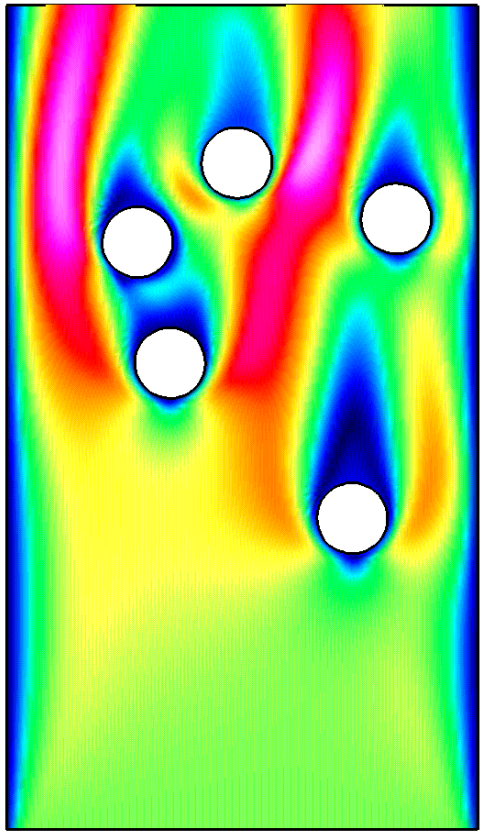

- Overlapping grids can be rapidly generated as bodies move.
- High quality grids under large displacements.
- Cartesian grids for efficiency.
- Efficient for high-order accurate methods.

What are overlapping grids and why are they useful?

Overlapping grid: a set of structured grids that overlap.

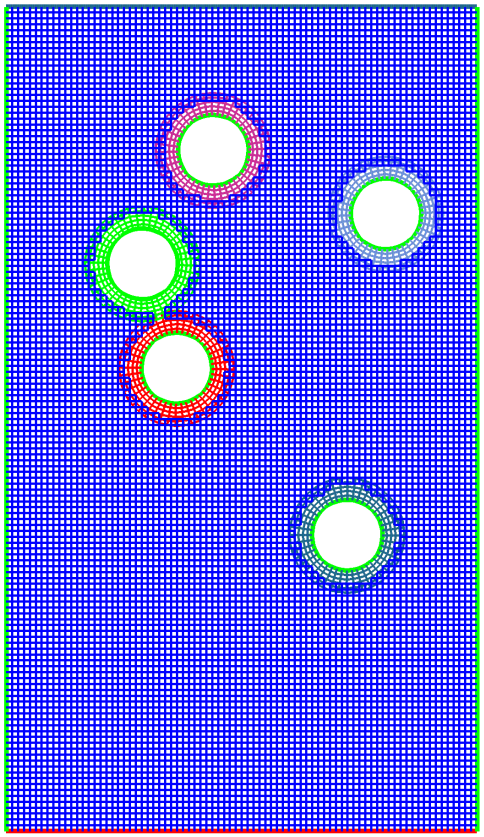

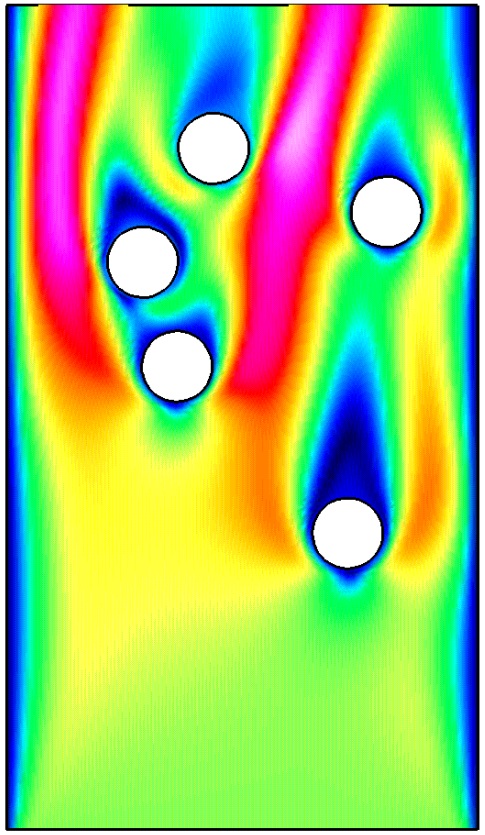

- Overlapping grids can be rapidly generated as bodies move.
- High quality grids under large displacements.
- Cartesian grids for efficiency.
- Efficient for high-order accurate methods.

Deforming composite grids (DCG) for Fluid-Structure Interactions (FSI)

Goal: To perform coupled simulations of compressible fluids and deforming solids.

A mixed Eulerian-Lagrangian approach:

- Fluids: general moving coordinate system with overlapping grids.
- Solids : fixed reference frame with overlapping-grids (later: unstructured-grids, or beam/plate models).
- Boundary fitted deforming grids for fluid-solid interfaces.

Strengths of the approach:

- maintains high quality grids for large deformations/displacements.
- efficient structured grid methods (AMR) optimized for Cartesian grids.

A sample FSI-DCG simulation

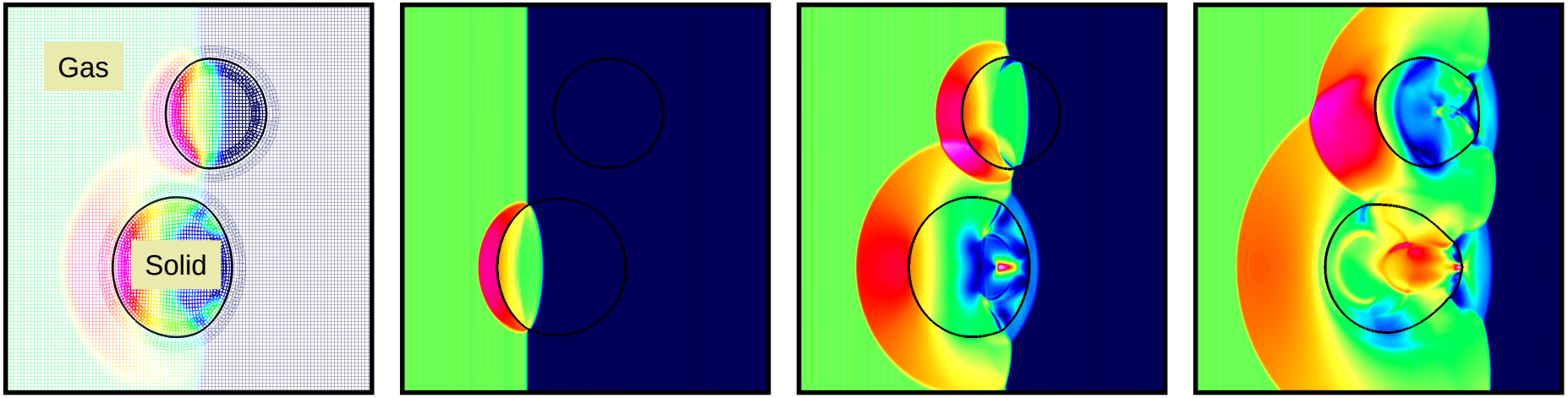

Mach 2 shock in a gas hitting two elastic cylinders.

- Solve Euler equations in the fluid domains on moving grids.
- Solve equations of linear elasticity in the solid domains.
- Fluid grids at the interface deform over time (hyperbolic grid generator).
- Adaptive mesh refinement (in progress).

Fluid and Solid Solvers

Fluid solver: we solve the inviscid Euler equations with a second-order extension of Godunov's method (cgcns).

- WDH., D. W. Schwendeman, *Parallel Computation of Three-Dimensional Flows using Overlapping Grids with Adaptive Mesh Refinement*, J. Comp. Phys. **227** (2008).
- WDH., DWS, *Moving Overlapping Grids with Adaptive Mesh Refinement for High-Speed Reactive and Nonreactive Flow*, J. Comp. Phys. **216** (2005).
- WDH., DWS, An adaptive numerical scheme for high-speed reactive flow on overlapping grids, J. Comp. Phys. **191** (2003).

Solid solver: we solve the elastic wave equation as a first order system with a second-order upwind characteristic scheme (cgsm).

- Daniel Appelö, JWB, WDH, DWS, *"Numerical Methods for Solid Mechanics on Overlapping Grids: Linear Elasticity*, LLNL-JRNL-422223, submitted (2010).

The elastic piston - a 1D FSI model problem

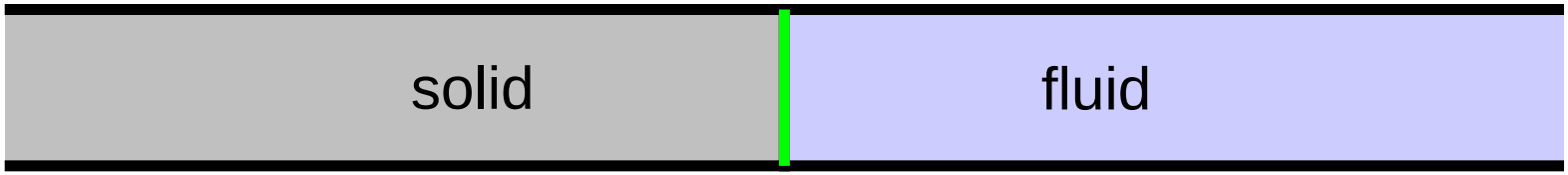

$\bar{\rho}$: density	ρ : density
$\bar{u}$: displacement	
$\bar{v}$: velocity	v : velocity
$\bar{\sigma}$: stress	$\sigma = -p$: stress, pressure
c_p : speed of sound	a : speed of sound
$\bar{z} = \bar{\rho} c_p$: impedance	$z = \rho a$: impedance

The elastic piston

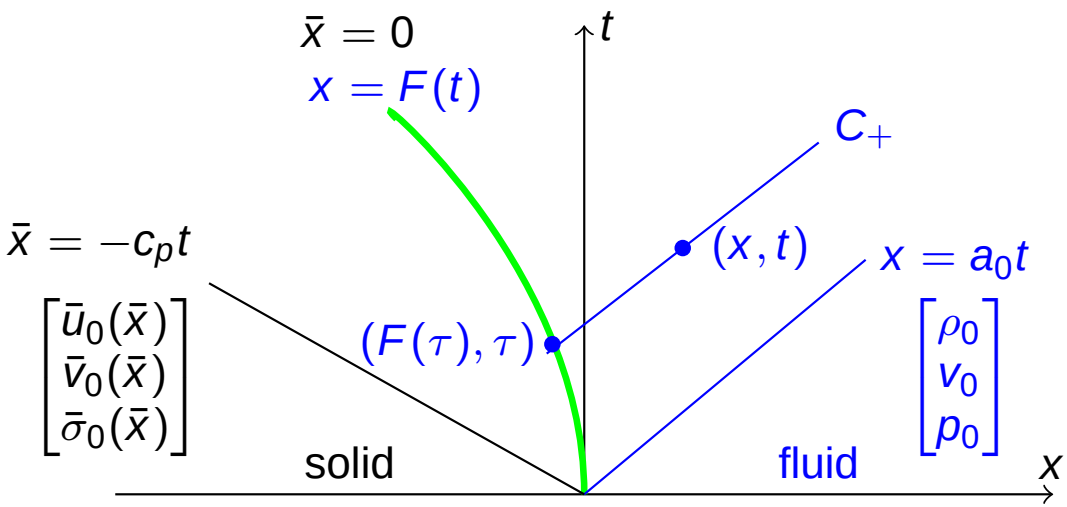

The governing equations for the solid and fluid are

$$\begin{cases} \bar{u}_t - \bar{v} = 0 \\ \bar{v}_t - \bar{\sigma}_{\bar{x}}/\bar{\rho} = 0 \\ \bar{\sigma}_t - \bar{\rho} c_p^2 \bar{v}_{\bar{x}} = 0 \end{cases}, \quad \text{for } \bar{x} < 0, \qquad \begin{cases} \rho_t + (\rho v)_x = 0 \\ (\rho v)_t + (\rho v^2 + p)_x = 0 \\ (\rho E)_t + (\rho E v + p v)_x = 0 \end{cases}, \quad \text{for } x > F(t),$$

where $\rho E = p/(\gamma - 1) + \rho v^2/2$. The interface conditions are

$$\bar{v}(0, t) = v(F(t), t),$$
$$\bar{\sigma}(0, t) = \sigma(F(t), t) \equiv -p(F(t), t) + p_e.$$

The elastic piston

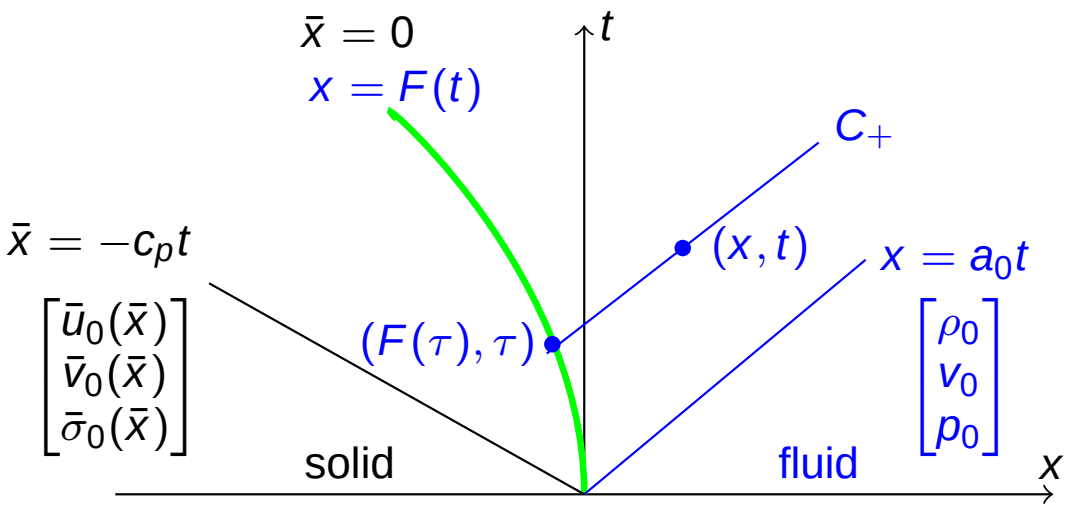

The governing equations for the solid and fluid are

$$\begin{cases} \bar{u}_t - \bar{v} = 0 \\ \bar{v}_t - \bar{\sigma}_{\bar{x}}/\bar{\rho} = 0 \\ \bar{\sigma}_t - \bar{\rho} c_p^2 \bar{v}_{\bar{x}} = 0 \end{cases}, \quad \text{for } \bar{x} < 0, \qquad \begin{cases} \rho_t + (\rho v)_x = 0 \\ (\rho v)_t + (\rho v^2 + p)_x = 0 \\ (\rho E)_t + (\rho E v + p v)_x = 0 \end{cases}, \quad \text{for } x > F(t),$$

where $\rho E = p/(\gamma - 1) + \rho v^2/2$. The interface conditions are

$$\bar{v}(0, t) = v(F(t), t),$$
$$\bar{\sigma}(0, t) = \sigma(F(t), t) \equiv -p(F(t), t) + p_e.$$

An exact solution to the elastic piston problem

For a given $x = F(t)$, and constant $\rho_0, p_0, v_0 = 0$, the solution in the fluid region $F(t) < x < a_0 t$ is (assuming no shocks)

$$v(x,t) = \dot{F}(\tau(x,t)), \quad \frac{a(x,t)}{a_0} = 1 + \frac{\gamma - 1}{2}\left(\frac{v(x,t)}{a_0}\right), \quad \frac{p(x,t)}{p_0} = \left(\frac{\rho(x,t)}{\rho_0}\right)^{\gamma} = \left(\frac{a(x,t)}{a_0}\right)^{2\gamma/(\gamma-1)},$$

$$x - F(\tau) = \left[a_0 + \frac{\gamma+1}{2}\dot{F}(\tau)\right](t - \tau).$$

The general solution for the solid follows from the d'Alembert solution,

$$\bar{u}(\bar{x},t) = f(\bar{x} - c_p t) + g(\bar{x} + c_p t),$$

$$f(\xi) = \frac{1}{2}\left[\bar{u}_0(\xi) - \frac{1}{c_p}\int_0^{\xi} \bar{v}_0(s)ds\right] \quad \text{for } \xi < 0,$$

$$g(\xi) = \begin{cases} \frac{1}{2}\left[\bar{u}_0(\xi) + \frac{1}{c_p}\int_0^{\xi} \bar{v}_0(s)ds\right] & \text{for } \xi < 0, \\ F(\xi/c_p) - f(-\xi) & \text{for } \xi > 0. \end{cases}$$

Applying the interface equations gives an ODE for $F(t)$ in terms of the initial conditions,

$$\frac{p_0}{\bar{\rho}c_p^2}\left[1 + \frac{\gamma-1}{2a_0}\dot{F}(t)\right]^{2\gamma/(\gamma-1)} + \frac{\dot{F}(t)}{c_p} = -\left[\bar{u}_0'(-c_p t) - \frac{1}{c_p}\bar{v}_0(-c_p t)\right], \quad \text{for } t > 0.$$

Alternatively if we choose $F(t) = -\frac{a}{q}t^q$, we can choose initial conditions in the solid as

$$\bar{u}_0(\bar{x}) = -\frac{p_0}{\bar{\rho}_0 c_p^2}\int_0^{\bar{x}}\left[1 + \frac{\gamma-1}{2a_0}\dot{F}(-s/c_p)\right]^{2\gamma/(\gamma-1)} ds, \qquad \bar{v}_0(\bar{x}) = \dot{F}(-\bar{x}/c_p), \quad \text{for } \bar{x} < 0,$$

to give a smooth solution with the specified interface motion.

The solution of the fluid-solid Riemann (FSR) problem defines our interface projection.

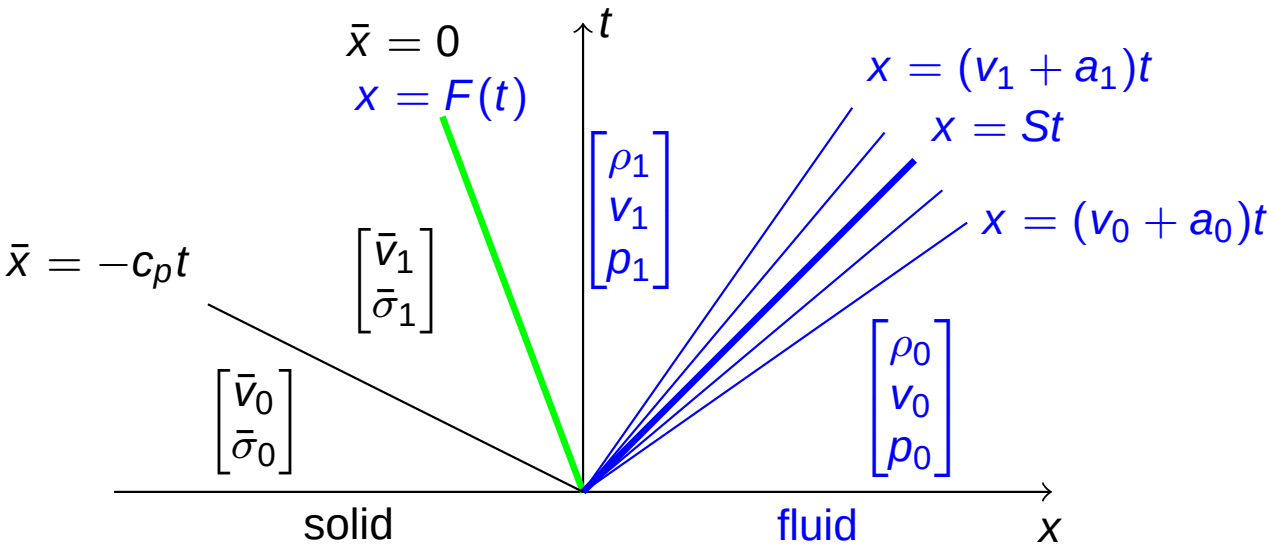

- special case of elastic piston problem - constant initial conditions in fluid and solid.
- the fluid may have a shock or expansion fan on the $\mathcal{C}^+$ characteristic.

Solution of the linearized fluid-solid Riemann problem

Characteristic relations:

$$\begin{aligned} \text{Solid:} \quad & \bar{z}\bar{v} \mp \bar{\sigma} = \bar{z}\bar{v}_0 \mp \bar{\sigma}_0, \ \text{ on } d\bar{x}/dt = \pm c_p, \\ \text{Fluid:} \quad & zv \mp \sigma = zv_0 \mp \sigma_0, \ \text{ on } dx/dt = v_0 \pm a_0, \end{aligned}$$

where $z = \bar{\rho} c_p$ and $\bar{z} = \bar{\rho} a_0$ are the *acoustic impedances*.

The state next to the interface is an impedance weighted average of the fluid and solid states:

$$\begin{aligned} v_1 = \bar{v}_1 &= \frac{\bar{z}\bar{v}_0 + z v_0}{\bar{z} + z} + \frac{\sigma_0 - \bar{\sigma}_0}{\bar{z} + z}, \\ \sigma_1 = \bar{\sigma}_1 &= \frac{\bar{z}^{-1}\bar{\sigma}_0 + z^{-1}\sigma_0}{\bar{z}^{-1} + z^{-1}} + \frac{v_0 - \bar{v}_0}{\bar{z}^{-1} + z^{-1}}. \end{aligned}$$

The solution to the full nonlinear problem can also be determined.

The FSI-DCG time-stepping algorithm

The FSI-DCG interface approximation is an extension of the scheme of Banks and Sjögreen:

J. W. Banks and B. Sjögreen, *A Normal Mode Stability Analysis of Numerical Interface Conditions for Fluid/Structure Interaction*, Commun. Comput. Phys., 2011.

The main steps are:

1. The fluid and solid domains are first advanced independently giving provisional interface values.
2. The provisional interface values are projected based on the solution to the fluid-solid Riemann problem.

The FSI-DCG time-stepping algorithm

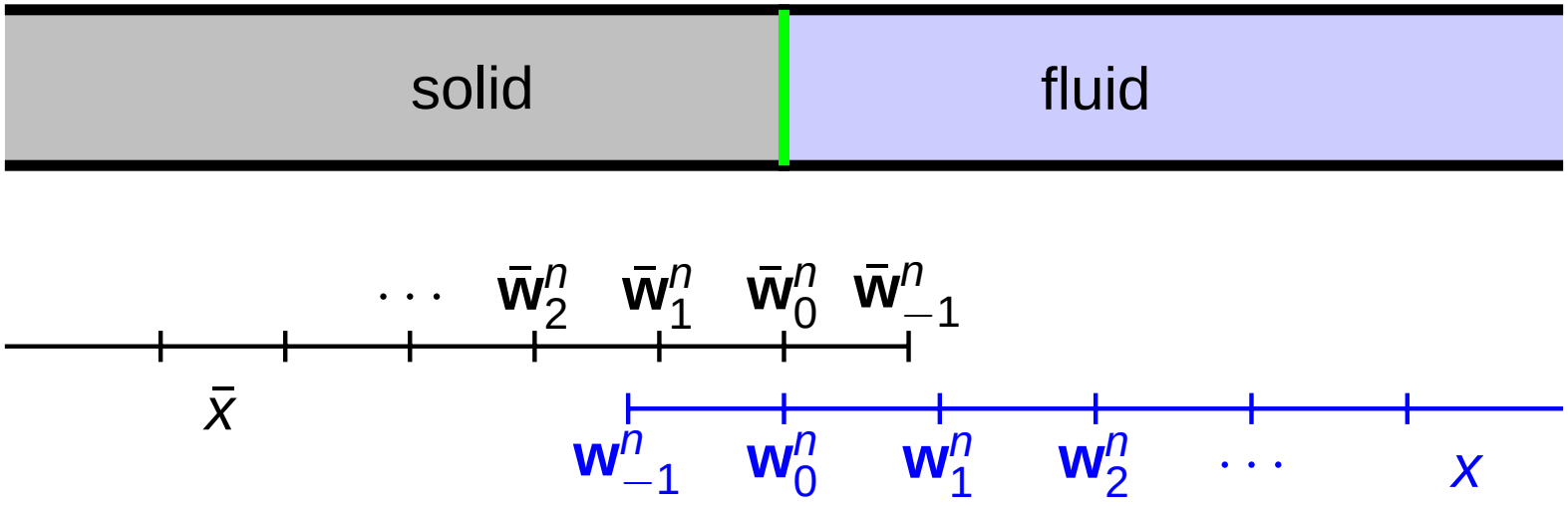

Define discrete approximations, ($v_i^n \approx v(i\Delta x_i, n\Delta t)$, $\bar{v}_i^n \approx \bar{v}(i\Delta \bar{x}_i, n\Delta t)$)

$$\text{Solid:} \quad \bar{\mathbf{w}}_i^n = [\bar{u}_i^n, \bar{v}_i^n, \bar{\sigma}_i^n] \qquad i = -1, 0, 1, \ldots$$

$$\text{Fluid:} \quad \mathbf{w}_i^n = [\rho_i^n, v_i^n, p_i^n], \qquad i = -1, 0, 1, \ldots$$

The FSI-DCG time-stepping algorithm

stage	condition	type	assigns
1a	Predict grid and grid velocity	extrapolation	F^p, $\dot{F}^p$
1b	Advance $\mathbf{w}_i^n$, $\bar{\mathbf{w}}_i^n$, $i = 0, 1, 2, \ldots$	PDE	interior, interface
2a	Eval v_I, σ_I, ρ_I from FSR	projection	v_I, σ_I, ρ_I
2b	$v_0^n, \bar{v}_0^n = v_I$, $-p_0^n, \bar{\sigma}_0^n = \sigma_I$, $\rho_0^n = \rho_I$	projection	$\mathbf{w}_0^n$, $\bar{\mathbf{w}}_0^n$
2c	$\mathbf{w}_{-1}^n = \mathcal{E}_{+1}^{(3)}\mathbf{w}_0^n$, $\bar{\mathbf{w}}_{-1}^n = \bar{\mathcal{E}}_{+1}^{(3)}\bar{\mathbf{w}}_0^n$,	extrapolation	$\mathbf{w}_{-1}^n$, $\bar{\mathbf{w}}_{-1}^n$
2d	Eval : $\dot{v}_f = -\frac{1}{\rho}\partial_x p, \ldots$	PDE	$\dot{v}_f$, $\dot{v}_s$, $\dot{\sigma}_f$, $\dot{\sigma}_s$
2e	Eval $\dot{v}_I$, $\dot{\sigma}_I$ from FSR	projection	$\dot{v}_I$, $\dot{\sigma}_I$
3a	$-\frac{1}{\rho}\partial_x p = \dot{v}_I$, $\rho a^2 \partial_x v = \dot{\sigma}_I$	compatibility	p_{-1}^n, v_{-1}^n
3b	$\bar{\rho} c_p^2 \partial_x \bar{v} = \dot{\sigma}_I$, $\frac{1}{\bar{\rho}}\partial_x \bar{\sigma} = \dot{v}_I$	compatibility	$\bar{v}_{-1}^n$, $\bar{\sigma}_{-1}^n$
3c	Correct grid and grid velocity	projection	F^n, $\dot{F}^n$

The interface projection step

Using the linearized FSR solution, the interface values are an impedance weighted average of the provisional fluid and solid values:

$$v_I = \frac{\bar{z}\bar{v}_0 + z v_0}{\bar{z} + z} + \frac{\sigma_0 - \bar{\sigma}_0}{\bar{z} + z},$$
$$\sigma_I = \frac{\bar{z}^{-1}\bar{\sigma}_0 + z^{-1}\sigma_0}{\bar{z}^{-1} + z^{-1}} + \frac{v_0 - \bar{v}_0}{\bar{z}^{-1} + z^{-1}}$$

Compare: the *standard* FSI scheme uses the *heavy solid* limit, $\bar{z} \gg z$, *velocity-from-solid, stress-from-fluid*:

$$v_I = \bar{v}_0$$
$$\sigma_I = \sigma_0 = -p + p_e$$

The standard scheme is unstable for *light* solids.

Note: for hard problems with shocks hitting the interface, there are advantages to using the full nonlinear solution to the FSR problem.

Elastic piston numerical results

Computed solution for a smoothly receding piston.

		Fluid						Solid					
grid	N	ρ	r	v	r	p	r	$\bar{u}$	r	$\bar{v}$	r	$\bar{\sigma}$	r
G_1	20	2.2e-3		2.7e-3		1.6e-3		4.9e-4		9.3e-5		1.2e-4	
G_2	40	5.4e-4	4.1	6.2e-4	4.3	3.7e-4	4.3	1.2e-4	4.2	2.6e-5	3.6	2.3e-5	5.0
G_3	80	1.4e-4	3.9	1.5e-4	4.0	9.3e-5	4.0	2.9e-5	4.1	6.2e-6	4.1	5.0e-6	4.7
G_4	160	3.5e-5	3.9	3.9e-5	3.9	2.3e-5	4.0	7.3e-6	4.0	1.5e-6	4.1	1.1e-6	4.4
rate		1.99		2.03		2.03		2.03		1.99		2.24	

Max-norm errors for very light solid: $\bar{\rho} = 10^{-5}$, $z/\bar{z} = 5.8 \times 10^3$.

		Fluid						Solid					
grid	N	ρ	r	v	r	p	r	$\bar{u}$	r	$\bar{v}$	r	$\bar{\sigma}$	r
G_1	20	9.2e-4		9.6e-4		8.5e-4		3.0e-4		1.3e-5		1.1e-5	
G_2	40	2.1e-4	4.3	2.3e-4	4.2	2.0e-4	4.2	7.3e-5	4.2	3.0e-6	4.4	2.6e-6	4.2
G_3	80	5.6e-5	3.8	5.6e-5	4.1	4.9e-5	4.1	1.8e-5	4.0	6.9e-7	4.4	6.3e-7	4.2
G_4	160	1.5e-5	3.9	1.4e-5	4.0	1.2e-5	4.0	4.5e-6	4.0	1.6e-7	4.2	1.5e-7	4.2
rate		1.99		2.04		2.04		2.02		2.12		2.07	

Max-norm errors for very heavy solid: $\bar{\rho} = 10^5$, $z/\bar{z} = 5.8 \times 10^{-7}$.

- Max-norm errors are converging to second-order accuracy.
- Scheme is stable for large and small impedance ratios.

Two-dimensional verification problems

1. superseismic shock.
2. deforming diffuser.

The superseismic shock FSI problem

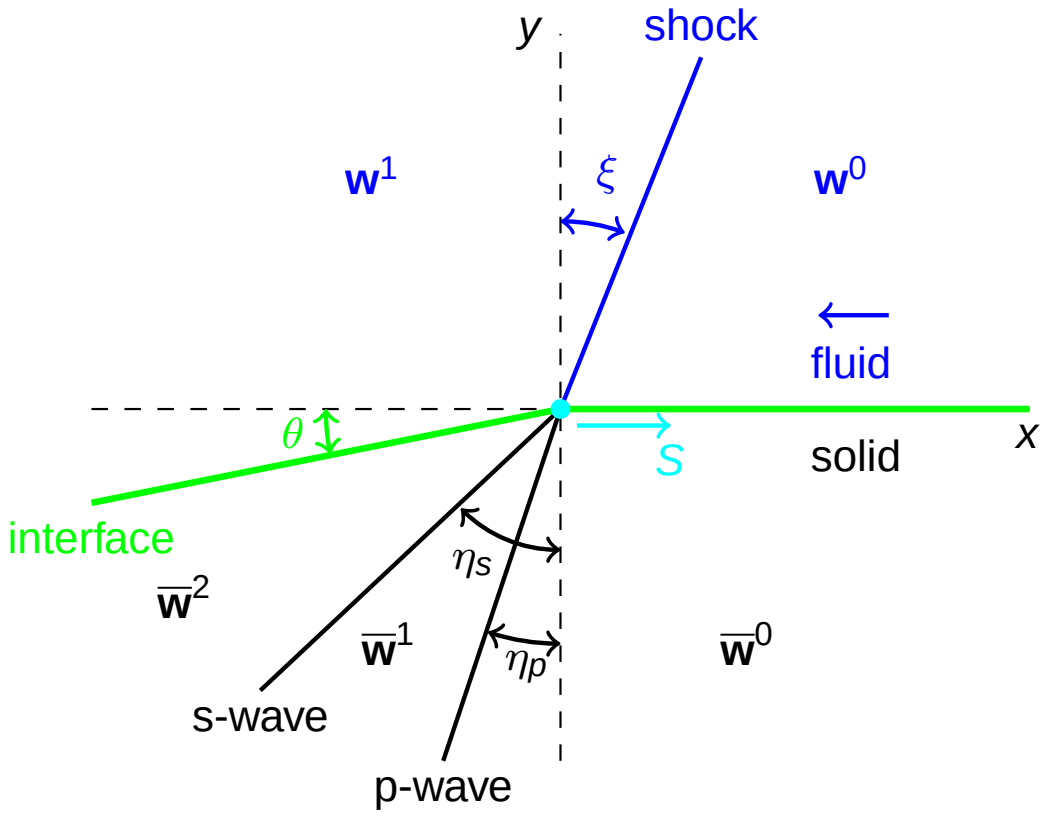

- a fluid shock moving from left to right deflects a solid interface.
- an FSI problem with an analytic traveling wave solution.

Superseismic shock: grids and computed solution

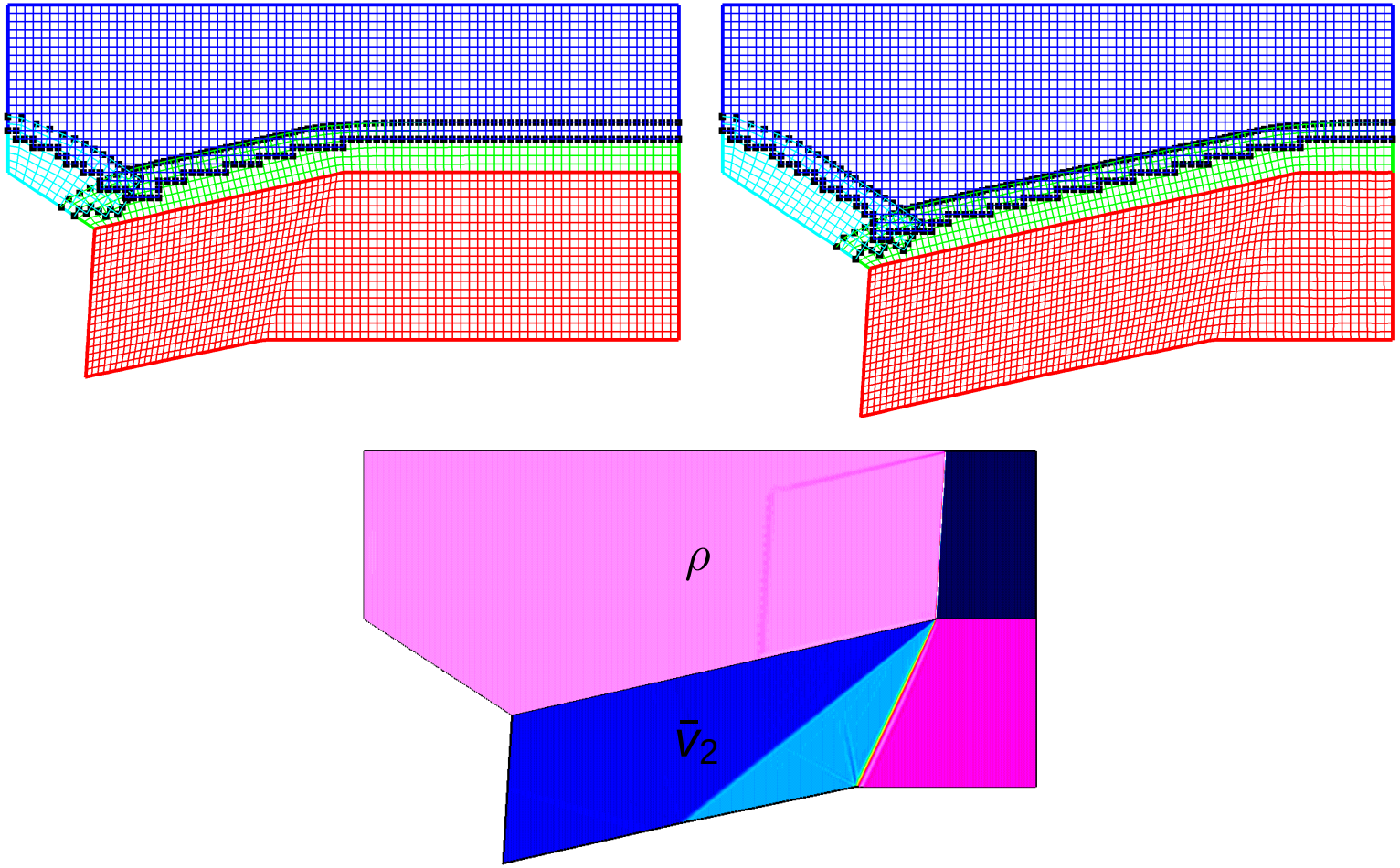

- The red grid for the solid domain is shown adjusted for the displacement.

L_1-norm errors and convergence rates for the superseismic shock

	Solid						Fluid					
Grid	$\lvert\bar{\mathbf{u}}\rvert$	r	$\lvert\bar{\mathbf{v}}\rvert$	r	$\lvert\bar{\boldsymbol{\sigma}}\rvert$	r	ρ	r	$\lvert\mathbf{v}\rvert$	r	T	r
$\mathcal{G}_{ss}^{(4)}$	8.6e-5		2.8e-3		7.9e-3		4.6e-3		2.2e-2		1.1e-2	
$\mathcal{G}_{ss}^{(8)}$	3.6e-5	2.4	1.7e-3	1.6	5.0e-3	1.6	2.6e-3	1.8	1.3e-2	1.7	6.6e-3	1.7
$\mathcal{G}_{ss}^{(16)}$	1.5e-5	2.5	1.1e-3	1.6	3.1e-3	1.6	1.4e-3	1.9	6.7e-3	1.9	3.5e-3	1.9
$\mathcal{G}_{ss}^{(32)}$	5.6e-6	2.7	6.9e-4	1.6	2.0e-3	1.6	7.0e-4	2.0	3.4e-3	2.0	1.7e-3	2.0
rate	1.32		0.67		0.67		0.91		0.92		0.91	

- Due to the discontinuities, the L_1-norm errors do not converge at second-order.
- The solid variables $\bar{v}$ and $\bar{\sigma}$ converge at the expected rates of $2/3$ (due to spreading of the linear discontinuities).
- In isolation the fluid domain should converge at first order.

The deforming diffuser

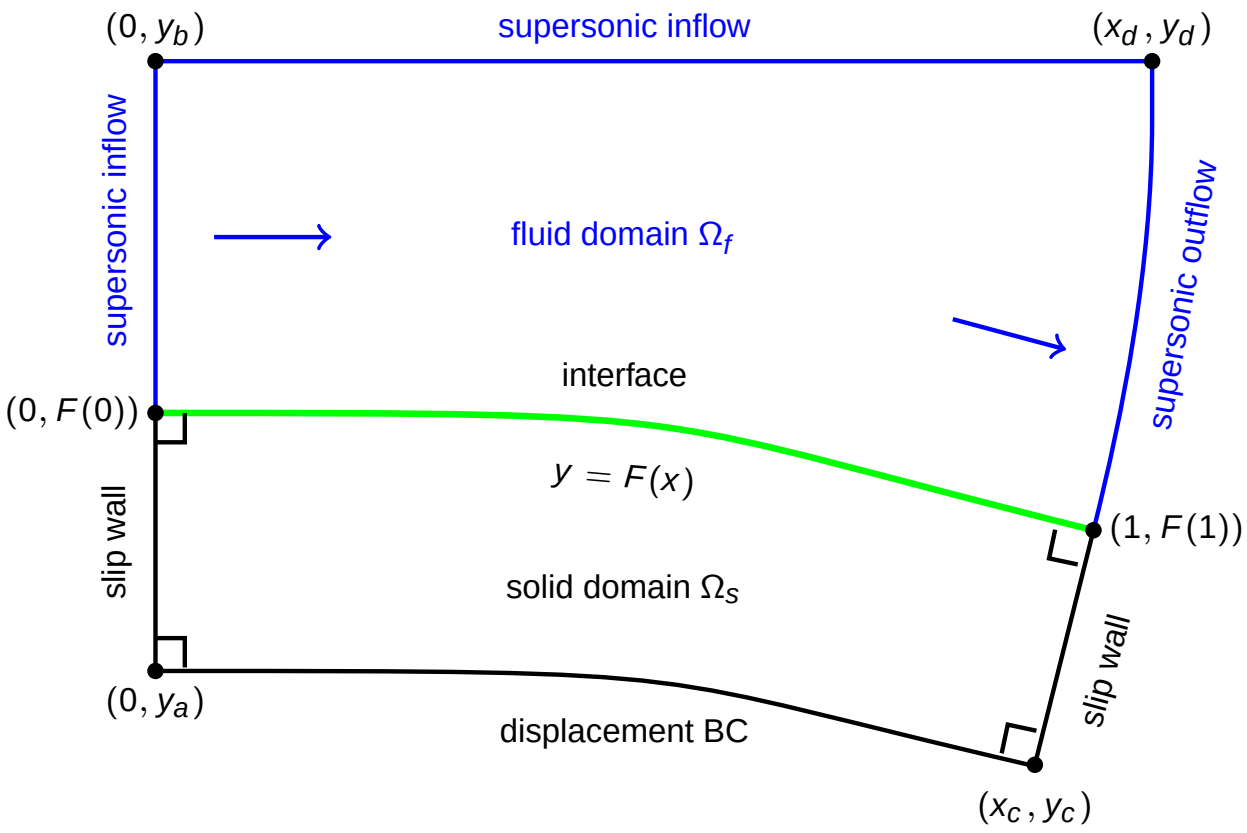

- an FSI problem with a smooth semi-analytic solution.
- Fluid: Prandtl-Meyer analytic solution is defined as a function of $F(x)$.
- Solid: steady elasticity equations are solved on a fine grid.
- The coupled *exact* solution and $F(x)$ are determined by iteration.

The deforming diffuser grid and solution

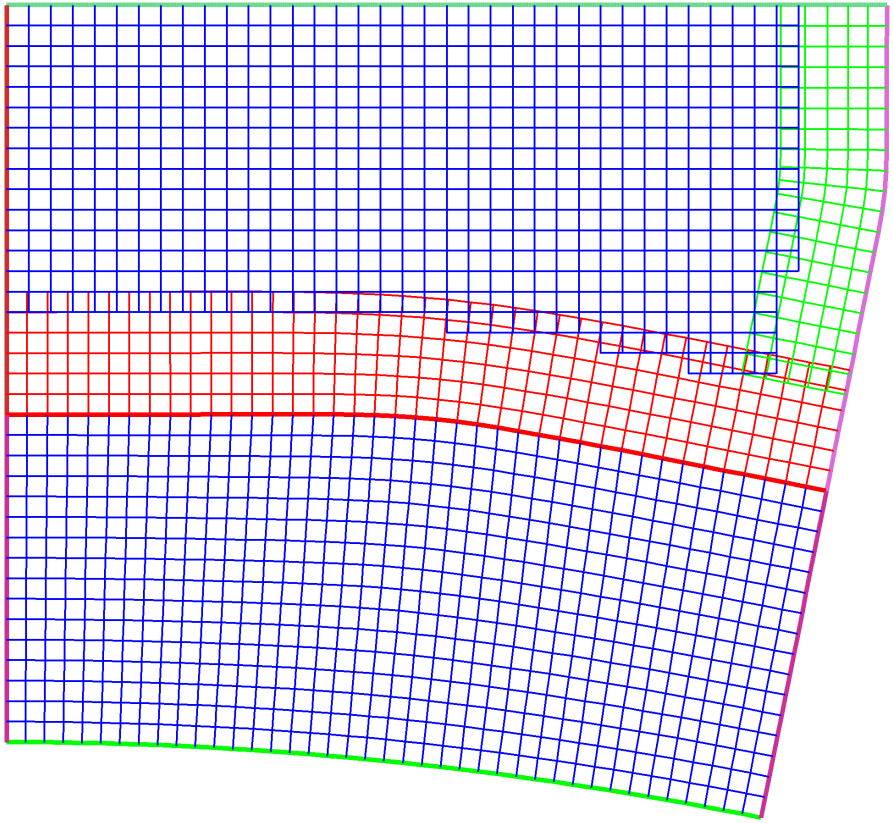

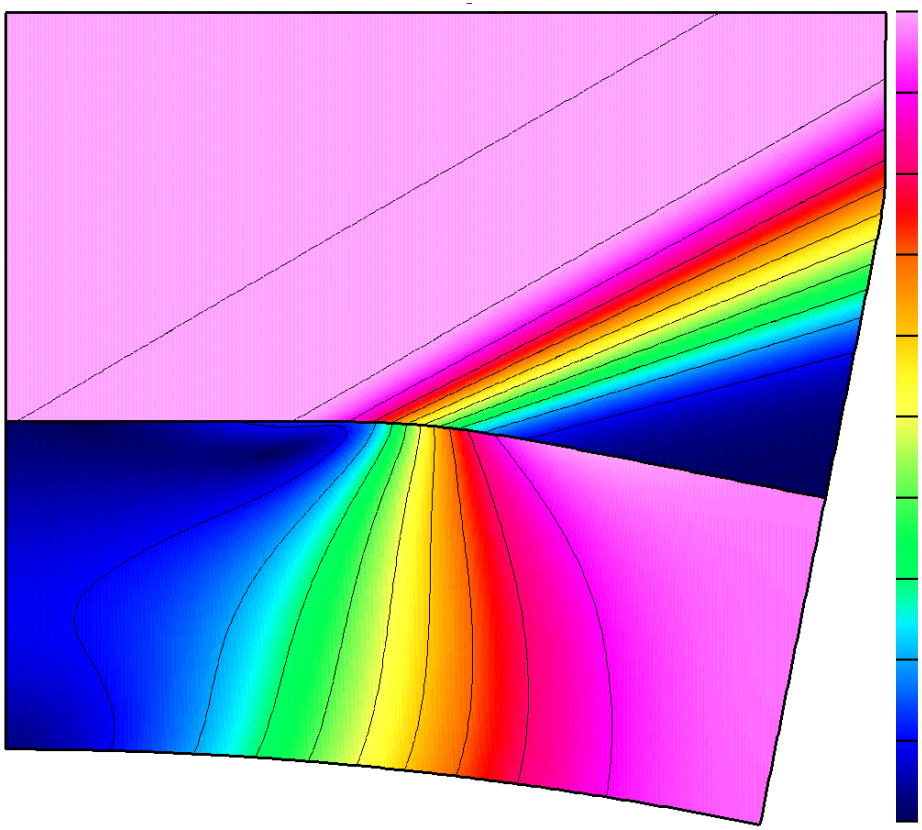

Contours of the fluid pressure, $[\min, \max] = [.5, 1.]$ and norm of the solid stress tensor $|\bar{\sigma}|$, $[\min, \max] = [0, .054]$.

Max-norm errors and convergence rates for the deforming diffuser

	Solid					
Grid	$\lvert\bar{\mathbf{u}}\rvert$	r	$\lvert\bar{\mathbf{v}}\rvert$	r	$\lvert\bar{\boldsymbol{\sigma}}\rvert$	r
$\mathcal{G}_{dd}^{(2)}$	2.3e-4		8.6e-4		4.0e-2	
$\mathcal{G}_{dd}^{(4)}$	5.8e-5	3.9	2.3e-4	3.8	1.2e-2	3.4
$\mathcal{G}_{dd}^{(8)}$	9.9e-6	5.9	4.6e-5	5.0	2.0e-3	5.8
$\mathcal{G}_{dd}^{(16)}$	1.6e-6	6.2	9.5e-6	4.8	3.4e-4	5.9
rate	2.40		2.18		2.31	

	Fluid							
Grid	ρ	r	v_1	r	v_2	r	T	r
$\mathcal{G}_{dd}^{(2)}$	3.6e-2		1.7e-2		2.3e-2		1.2e-2	
$\mathcal{G}_{dd}^{(4)}$	8.8e-3	4.1	3.8e-3	4.5	7.1e-3	3.2	2.5e-3	4.7
$\mathcal{G}_{dd}^{(8)}$	2.1e-3	4.1	8.6e-4	4.4	2.3e-3	3.1	7.9e-4	3.2
$\mathcal{G}_{dd}^{(16)}$	5.0e-4	4.3	2.0e-4	4.3	5.2e-4	4.5	1.7e-4	4.8
rate	2.05		2.15		1.80		2.02	

- max-norm errors at $t = 1$ with the Godunov slope-limiter off.
- solutions are converging to second-order in the max norm.

Summary

- the deforming composite grid (DCG) approach is being developed to to model fluid-structure interactions (FSI) for compressible fluids and elastic solids.
- the solution of the fluid-solid Riemann problem can be used to define stable interface approximations for both *light* and *heavy* solids.
- our FSI-DCG approximation was verfied to be second-order accurate in the max-norm on problems with smooth solutions.

Future work:

- support for adaptive mesh refinement (AMR) at the interface.
- more general solid mechanics models.
- incompressible fluids.
- extend to three space dimensions.